Effect of Hypotensive Brain Death on the Donor Liver and Its Mechanism in an Improved Bama Miniature Pig (*Sus scrofa domestica*) Model

N.-N. Wang[a], G.-N. Chen[a], B. Qu[a,*], F. Yu[b], G.-N. Sheng[c], and Y. Shi[c,*]

[a]Postgraduate Training Base, Affiliated Hospital of Logistics University of Chinese People's Armed Police Force, Jinzhou Medical University, Tianjin, China; [b]Department of Emergency, the Seventh Affiliated Hospital of Sun Yat-Sen University, Shenzhen, China; and [c]Organ Transplantation Center, Tianjin First Center Hospital, Nankai District, Tianjin, China

ABSTRACT

Background. We aimed to observe the effect of hypotensive brain death on the donor liver and understand its pathophysiological mechanism in improved pig model.

Methods. The model was induced using the modified intracranial water sac inflation method in 16 Bama miniature pigs. Effects of hypotensive brain death on liver function and tissue morphology were evaluated via changes in liver function enzyme index, liver tissue alkaline phosphatase levels, hourly bile flow, and liver tissue pathology. Its pathophysiological mechanism was examined on the basis of changes in portal vein blood flow, hepatic artery blood flow, portal venous endotoxin level, and liver tissue cytokine levels.

Results. After model establishment, portal vein blood flow, hepatic arterial blood flow, hourly bile flow, and alkaline phosphatase content in hepatic tissue significantly decreased, and serum aspartate aminotransferase, alkaline phosphatase, and lactate dehydrogenase levels significantly increased. Hematoxylin-eosin staining of liver tissue showed that after model establishment, hepatic tissue injury was gradually aggravated and hepatic cells were irreversibly damaged at 7 hours. Portal vein endotoxin levels significantly increased after brain death. Tumor necrosis factor α, interleukin 1, and endothelin 1 levels in liver tissues significantly increased at 3, 6, and 12 hours after brain death ($P < .05$), and hypoxia-inducible factor 1–α and nitric oxide levels significantly decreased ($P < .05$).

Conclusions. Hepatic injury was progressively aggravated under hypotensive brain death. The mechanism of donor liver injury under hypotensive brain death may involve low liver perfusion, release of intestinal endotoxin and inflammatory factors (eg, tumor necrosis factor α and interleukin 1), decreased hypoxia-inducible factor 1–α, and endothelin 1 and nitric oxide imbalance.

LIVER transplantation has become an effective treatment for various end-stage liver diseases. However, the number of patients awaiting liver transplantation is far greater than the number of available donor livers [1,2]. At present, donor livers mainly come from living donors, brain-dead donors (DBDs), and cardiac death donors (DCDs). Although the proportion of DCD organs increases every year, DBDs are still the main source of livers in the field of liver transplantation [1,3,4]. However, a series of pathophysiological changes (eg, hemodynamics, endocrine, metabolism, and inflammatory reaction) produced by brain

The first 2 authors contributed equally to this work.

*Address correspondence to Bo Qu, Department of Oncological Surgery, Affiliated Hospital of Logistics University of Chinese People's Armed Police Forces, No 220 Chenglin Rd, Dongli District, Tianjin 300162, China. Tel: +86-22-60578609; Fax: +86-22-60578609. E-mail: doctor_qb@163.com; and Yuan Shi, Organ Transplantation Center, Tianjin First Center Hospital, No 24 Fukang Rd, Nankai District, Tianjin 300192, China. E-mail: shiyuan_doctor@126.com

0041-1345/19
https://doi.org/10.1016/j.transproceed.2019.01.029

death, especially brain death coupled with circulation instability and hypotension for a long time, seriously affects the quality and immunocompetence of DBD livers, and using poor-quality organs would significantly affect the survival rate of transplant organs and long-term survival rate of recipients [5,6]. Hence, research on the effect of hypotensive brain death on donor livers has become a hot topic in the field of liver transplantation. However, the pathophysiological mechanism of the effect of hypotensive brain death on donor livers has not been fully elucidated [7].

In this study, we established a hypotensive brain death pig model, which is more stable and suitable for use in the field of transplantation, by using a modified intracranial water sac inflation method. Then, we observed the effects of brain death hypotension on the donor liver on the basis of changes in systemic hemodynamics, local hemodynamics of the liver, liver function, liver tissue pathology, liver tissue cytokine levels, and portal vein endotoxin level and further examined its pathophysiological mechanism.

MATERIALS AND METHODS

Ethics Approval

Sixteen female Bama miniature pigs (age, 10-12 months; weight, 30-40 kg) provided by the Tianjin Ji Xian Experimental Animal Center were investigated in the present study. Experimental procedures were performed in accordance with the guidelines of the Helsinki Convention and the Guide for the Care and Use of Laboratory Animals and were approved by the animal ethics committee of the Affiliated Hospital of Logistics University of Chinese People's Armed Police Forces.

Experiment Design

Baseline data were measured at the end of the animal preparation, and then the brain death hypotension model was induced. After the model was successfully established, the animals were monitored for 12 hours. At the end of the study, the animals were killed. T0 to T12 represent 0 to 12 hours after model establishment.

Animal Preparation

The animals fasted for 24 hours and were deprived of water for 12 hours before anesthesia. The animals received an intramuscular injection of 10 mg/kg ketamine, 0.4 mg/kg diazepam, and 0.03 mg/kg atropine. A blood oxygen saturation probe was connected to the pigs' tails, and 5 conduction electrocardiography monitoring electrodes were connected to the pigs' chests. The venous catheter was placed in the ear vein. The animals inhaled pure oxygen for 5 minutes through the animal mask and received an intravenous injection of 1 mg/kg ketamine and 1 mg/kg succinylcholine. Tracheal intubation was performed using No. 6.5 tracheal intubation and a 195-mm straight laryngoscope, and then the endotracheal intubation was connected to the anesthesia machine. Anesthesia was maintained by continuous inhalation of 2.5% to 3% sevoflurane and intravenous injection of 0.08 to 0.1 μg/(kg/h) remifentanil, and muscle relaxation was maintained by intermittent intravenous injection of vecuronium. A catheter was inserted into the external carotid artery to record the mean arterial pressure (MAP) and heart rate (HR). The catheter was inserted into the external jugular vein to record the central venous pressure and infuse fluid. Laparotomy was performed through a median incision of the abdomen and confirmed that the abdominal organs had no obvious lesions. The gallbladder was removed and the catheter inserted into the common bile duct to monitor bile flow. Blood flow probes were inserted into the portal vein and hepatic artery, which were connected to a flowmeter. After bladder puncture catheterization, the abdominal wall was closed.

The animal was adjusted to the prone position and sphenotresia was performed 1 cm behind the intersection of the ligature of the binoculus and sagittal line. Dura mater around the bone window was bluntly separated from the skull, and a No. 14 Foley water sac catheter was then placed. The bone window was closed using bone wax. Sphenotresia was performed 2 cm to the right of and 1 cm behind the previous hole. A Codman brain tissue intracranial pressure (ICP) monitoring probe was placed and connected to the ICP monitor, which was 2.5 cm from the outer edge of the skull. Eight needle electrodes that were connected to the physiological signal recording and analysis system were placed using the same method for electroencephalography (EEG) monitoring.

Establishment of a Hypotensive Brain Death Model

Normal saline was injected in the intracranial balloon catheter at a rate of 0.5 mL/min using a peristaltic pump. Pressurization was started when the MAP was greater than the ICP and then stopped when the ICP was greater than the MAP. Pressure adjustment was continued until the MAP no longer increased with increasing ICP. Brain death was confirmed when the model met the following 7 criteria: 1. remained in deep coma even after 1 hour from discontinuation of the anesthetic; 2. had moderately or completely dilated pupils and showed no corneal reflection and light reflex; 3. stopped spontaneous breathing and had a negative spontaneous breathing-induced test result; 4. presented a resting potential of >30 minutes on conduction EEG; 5. had an atropine test result; 6. showed oscillatory waves and sharp and small contraction waves in the anterior and posterior circulation on transcranial Doppler imaging; and 7. showed no changes in characteristics 1 to 6 over a 12-hour period [8,9].

Monitoring, Sampling, and Measurements

During the study, MAP was kept at > 60 mm Hg; central venous pressure, 8 to 12 mm Hg; arterial oxygen saturation, > 95%; $PaCO_2$, 35 to 45 mm Hg; and body temperature, > 36°C as much as possible. The HR, MAP, portal venous blood flow, hepatic arterial blood flow, and hourly bile flow were recorded respectively at baseline and T0 to T12. At baseline and T0 to T12, venous blood was extracted from the central venous catheter to detect alanine aminotransferase (ALT), aspartate aminotransferase (AST), alkaline phosphatase (ALP), and lactate dehydrogenase (LDH) levels using an automatic biochemical analyzer. Liver tissue was taken at baseline and T0 to T12 and divided into 3 portions: the first portion was stained with hematoxylin-eosin and analyzed by microscopy, the second portion was stained with acetic acid oil and lead citrate and observed by electron microscopy, and the third portion was frozen in liquid nitrogen and stored in a cryogenic refrigerator at −80°C. Using enzyme-linked immunosorbent assay kits (TSZ, San Francisco, Calif, United States), the levels of tumor necrosis factor α (TNF-α), interleukin 1 (IL-1), adenosine triphosphate (ATP), hypoxia-inducible factor 1−α (HIF-1α), endothelin 1 (ET-1), and nitric oxide (NO) were measured in accordance with the manufacturer's instructions. At baseline and T0 to T12, a blood sample (1-2 mL) was extracted from the portal vein using a sterile airtight centrifuge tube containing a small amount of anticoagulant to determine the bacterial endotoxin level with a quantitative analysis reagent kit of bacterial endotoxin limulus (TSZ) in accordance with the manufacturer's instructions.

Statistical Analyses

All data are presented as mean (SD). Baseline and T0 to T12 values were compared using a paired sample t test. A P value $< .05$ was considered statistically significant. All analyses were performed using SPSS Statistics Version 21.0 for Windows (IBM Corp, Armonk, NY, United States).

RESULTS

Of the 16 animals, 1 died of narcotic accident and 1 died of cerebral hemorrhage. Fourteen animals successfully completed the establishment of a hypotensive brain death model and survived until the end of the study.

EEG and Intracranial Blood Flow

Brainwave was normal and present at baseline and presented a resting state at T0 (Fig 1A). Transcranial Doppler imaging revealed that the anterior and posterior circulations consisted of normal waves at baseline and a T-wave spectrum at T0 (Fig 1B).

Changes in the Systemic and Hepatic Perfusions

Compared with the baseline values, the changes in HR at T0, T1, and T2 were not significant. After T2, HR increased rapidly and fluctuated significantly. Compared with the baseline value, the HR at T3, T4, T5, T6, T7, T8, T10, and T12 increased significantly ($P < .05$; Fig 2A). After model establishment, the animal MAP showed a downward trend. Compared with the baseline MAP, the MAP at T0 and the subsequent time points was significantly reduced ($P < .05$; Fig 2B). After model establishment, the blood flow in the portal vein and hepatic artery showed a decreasing trend. Compared with the baseline blood flow, the blood flow in the portal vein and hepatic artery were significantly reduced at T0 and subsequent time points ($P < .05$; Fig 2C).

Changes in Liver Function

Serum AST, LDH, ALP, and ALT levels showed elevated trends after model establishment. Compared with baseline values, serum AST and LDH levels were significantly increased at T0 and subsequent time points ($P < .05$), and serum ALP level was significantly increased at T0, T5, and subsequent time points ($P < .05$). Serum ALT level was significantly elevated at T9 ($P < .05$) and slightly elevated at all other time points ($P > .05$; Fig 3A, 3B). The ATP content in liver tissue fluctuated significantly after model establishment. Compared with the baseline value, the ATP content in liver tissue was significantly reduced at T3, T6, and T12 ($P < .05$; Fig 3C). After model establishment, the amount of hourly bile flow showed a decreasing trend. Compared with the baseline value, the hourly bile flow decreased significantly at T1, T3, and subsequent time points ($P < .05$; Fig 3D).

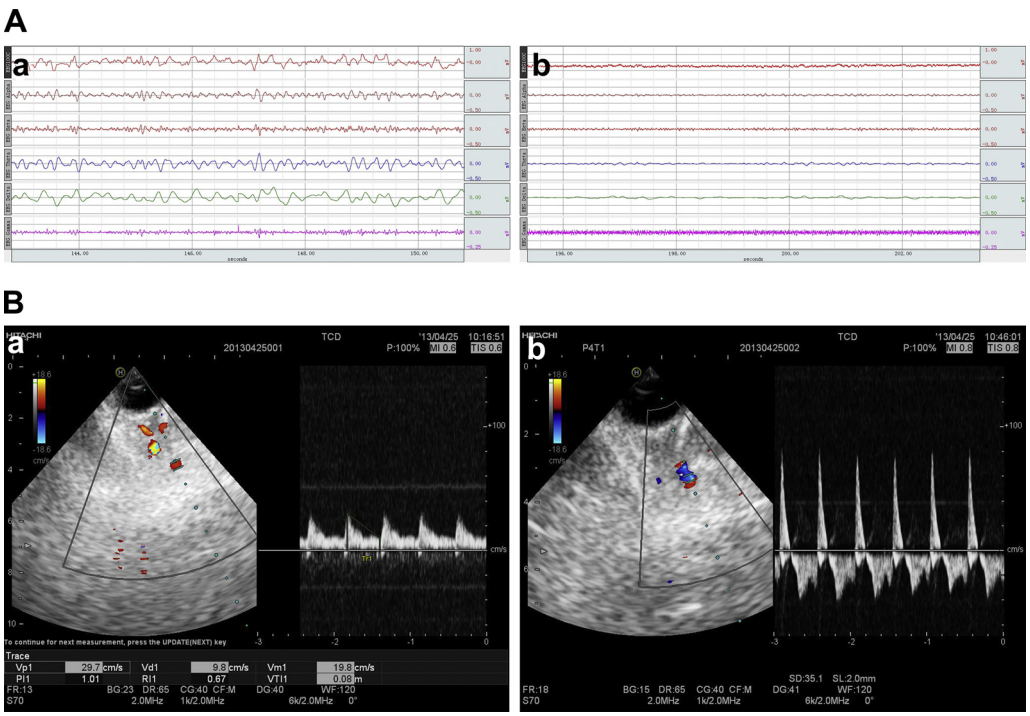

Fig 1. Electroencephalograms and transcranial Doppler images of the intracranial blood flow spectrum. (A) Electroencephalograms: (a) presence of brain electrical activity at baseline and (b) absence of brain electrical activity at T0. (B) Transcranial Doppler images of the intracranial blood flow spectrum: (a) normal spectrum at baseline and (b) T-wave spectrum at T0.

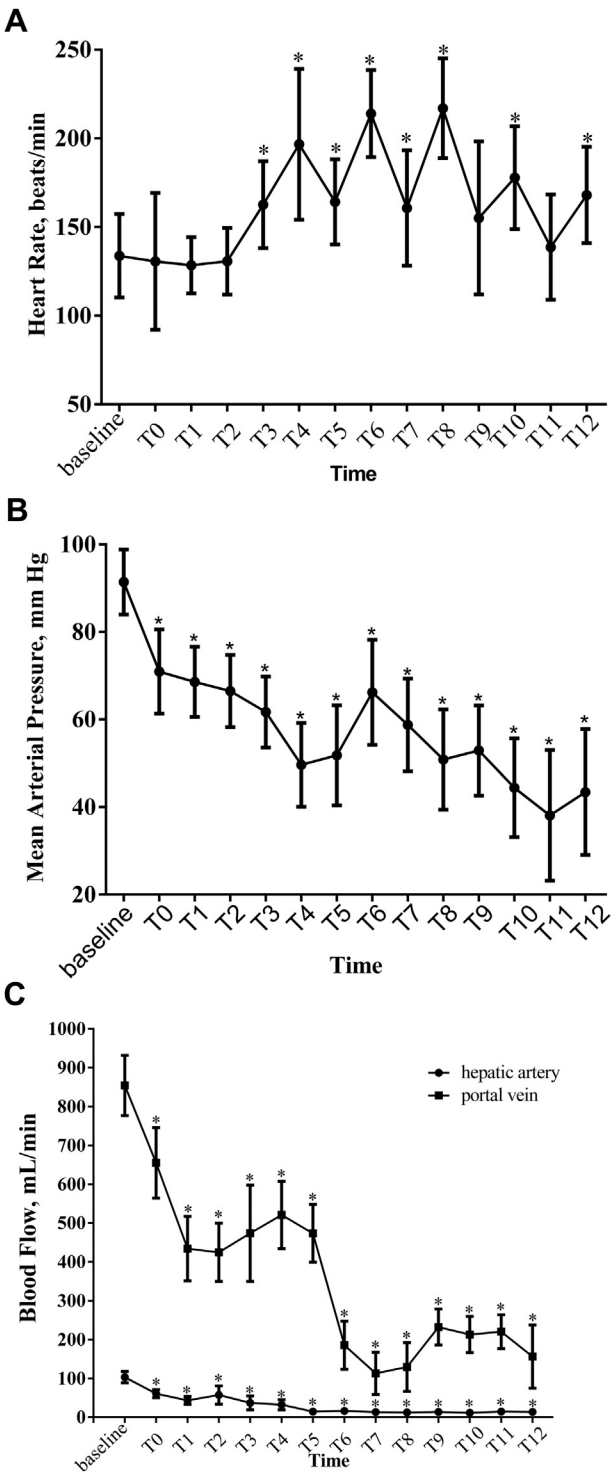

Fig 2. Changes in hemodynamics during the study. Data are expressed as mean (SD). Compared with the baseline, $^{*}P < .05$. (A) Changes in heart rate during the study; (B) changes in mean arterial pressure during the study; and (C) changes in hepatic arterial and portal vein flow during the study.

Changes in Cytokine and Endotoxin Levels

After model establishment, the levels of TNF-α, IL-1, and ET-1 in liver tissues and the endotoxin level in the portal vein showed increasing trends, and the HIF-1α and NO levels in liver tissues gradually decreased. Compared with baseline values, the TNF-α, IL-1, and ET-1 levels in liver tissues were significantly increased at T3, T6, and T12 ($P < .05$), and the HIF-1α and NO levels in liver tissues were significantly decreased at T3, T6, and T12 ($P < .05$; Table 1). The endotoxin level in the portal vein increased significantly at T2 and subsequent time points ($P < .05$; Fig 4).

Changes in Liver Tissue Morphology

The results of the liver tissue hematoxylin-eosin staining were as follows: at baseline, the liver cells without degeneration and edema showed a normal pattern of arrangement and morphology, and no inflammatory cells were observed. The hepatic cord was normal and the capsule was intact. At T1, the structure of the liver tissue was close to normal, and the liver cells had mild hydropic and vesicular fatty degenerations. At T2, the interlobular veins were congested. At T3, nuclear vacuoles could be seen in partial hepatocytes. At T4, interstitial hemorrhage in the portal area, moderate hepatocyte degeneration, partial hepatic sinus congestion, and eosinophilic changes in scattered hepatocytes were observed. At T5 and T6, interlobular vein expansion in the portal area and portal area edema were found. Hepatocytes with moderate watery degeneration and microvesicular fat presented diffuse distribution, and the large vesicular fatty degeneration and apoptosis presented a dispersed distribution. The liver sinus was compressed and the gap in the liver sinus was narrowed. At T7, scattered hepatocyte balloon degeneration and irreversible liver damage appeared. At T8 to T11, the irreversible liver damage gradually deteriorated. At T12, the hepatic cells showed multiple foci of large vesicular steatosis (Fig 5A).

Liver tissue electron microscopy revealed no fat vacuoles or nuclear deformation and no significant swelling of the mitochondrial membrane structure but showed an endoplasmic reticulum at baseline. The cell structure at T3 showed no significant difference with the one observed at baseline, but its arrangement was not as regular as that of normal liver cells. A few fat vacuoles could be observed at T3. At T12, several fat vacuoles of varying sizes were visible, and the organelle structure was vague. The mitochondria were swollen at T12 (Fig 5B).

DISCUSSION

Establishment of a Hypotensive Brain Death Pig Model

Currently, brain death animal models include rats, pigs, rabbits, cats, and sheep, among which pigs and rats are more commonly used [10–14]. In terms of the induction method for the brain death animal model, the most recent application is the classic epidural water sac inflation method

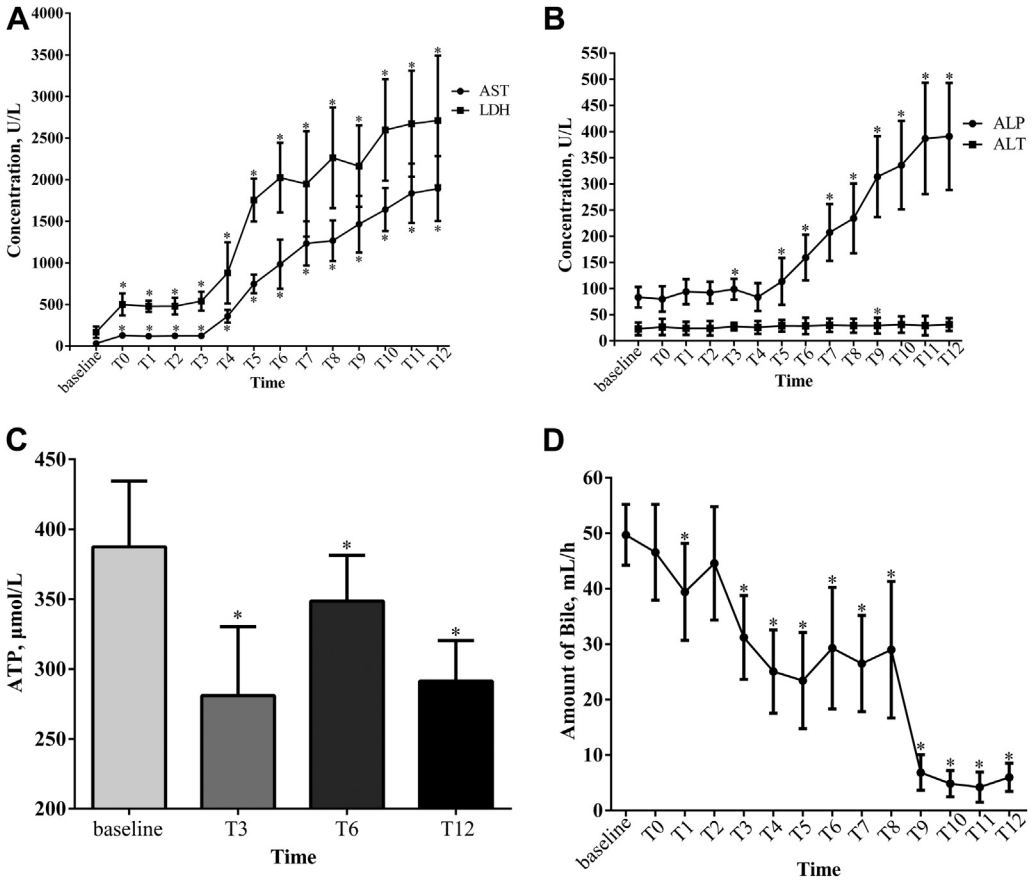

Fig 3. Changes in hepatic function during the study. Data are expressed as mean (SD). Compared with the baseline, $^{*}P < .05$. (A) Changes in aspartate aminotransferase (AST) and lactate dehydrogenase (LDH) levels in venous blood during the study; (B) changes in alanine aminotransferase (ALT) and alkaline phosphatase (ALP) levels in venous blood during the study; (C) changes in adenosine triphosphate (ATP) during the study; and (D) changes in the amount of bile per hour during the study.

[14–16]. The key to this modeling method is the rate and amount of water injection. However, differences in the water injection rate and water injection amount and adaptation of a continuous constant speed-pressurized strategy, which are reported in the literature, previously caused marked individual differences among the established brain death animal models; thus, these models cannot be used to accurately assess the body's physiological and biochemical changes after brain death [17–19]. We therefore improved the classic epidural water sac inflation method. Its core concept was that under the guidance of ICP and MAP, water was slowly discontinuously injected using a peristaltic pump to increase ICP. This can prevent not only a very fast and/or high increase in intracranial pressure, which can cause unnecessary damage to the brain, but also an excessive fluctuation of intracranial pressure, which can, in turn, cause excessive fluctuations of the cycle and cardiac functions.

In this study, in all 14 surviving animals, a hypotensive brain death model was successfully established, and monitoring indicators such as HR, electrocardiography, MAP, and ICP showed that the induction process was stable.

Table 1. Cytokine Concentration in Liver Tissue

	Baseline	T3	T6	T9
TNF-α	218.60 (23.77)	259.57 (39.81)*	267.50 (41.08)†	355.42 (53.37)†
IL-1	60.69 (14.00)	77.65 (8.21)†	84.05 (15.24)†	89.02 (13.40)†
ET-1	104.24 (16.30)	124.41 (22.65)†	135.18 (15.51)†	138.84 (25.30)†
NO	57.61 (16.57)	42.97 (14.25)*	38.76 (11.76)†	36.86 (7.38)†
HIF-α	34.63 (4.29)	28.97 (4.72)†	23.88 (6.69)†	19.21 (6.23)†

Abbreviations: ET-1, endothelin 1; HIF-1α, hypoxia-inducible factor 1–α; IL-1, interleukin 1; NO, nitric oxide; TNF-α, tumor necrosis factor α.
*$P < .05$ vs baseline.
†$P < .01$ vs baseline.

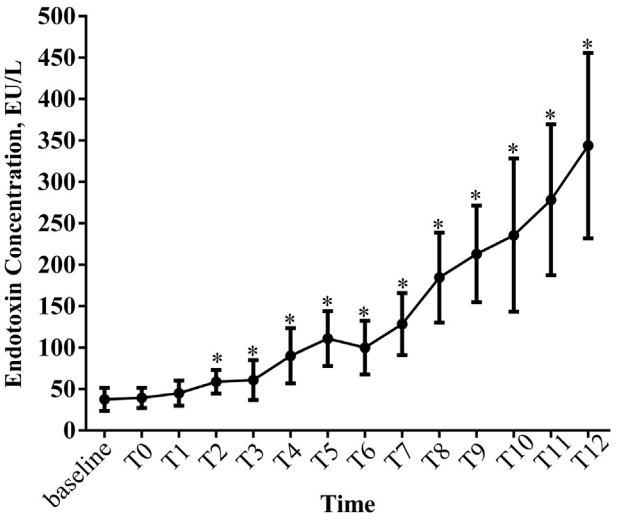

Fig 4. Changes in endotoxins during the study. Data are expressed as mean (SD). Compared with the baseline, $^{*}P < .05$.

Under real-time ICP and MAP monitoring, the hypotensive brain death pig model was successfully established using the slow and intermittent epidural water sac inflation method.

Effect of Hypotensive Brain Death on Liver Function and Liver Tissue Morphology

Under hypotensive brain death, serum AST, ALT, ALP, and LDH levels showed increasing trends, and AST and LDH levels significantly increased at T0 and each subsequent time point. The ALP levels significantly increased at T3, T5, and each subsequent time point, but ALT level changes were not significant. The hourly bile flow showed a decreasing trend and was significantly reduced at T1, T3, and each subsequent point. Liver function changed significantly 0 to 5 hours after hypotensive brain death, similar to the variation trend of the ALT, AST, and LDH levels observed by van Der Hoeven et al in a hypotensive brain death rat model [20]. The ATP content in hepatic tissue showed that the liver had an obvious energy metabolism disorder at T3. Novitzky et al found that brain death could induce anaerobic metabolism, elevate serum lactate level, and reduce ATP level [21]. However, Olinga et al found no significant difference in the liver ATP level between brain-dead rats and healthy rats [22]. No significant change in liver tissue pathology was observed 3 hours after hypotensive brain death, and the reversible damage increased gradually 3 to 6 hours after hypotensive brain death. Irreversible liver damage occurred at T7 and gradually increased after that. Electron microscopy revealed that compared with baseline observations, there were no significant changes at T3 and severe damage occurred at T12. Van der Hoeven et al found that the status of hypotensive brain death could induce progressive damage to the quality of donor livers in rats [23].

This study suggests that under the state of hypotensive brain death, hepatic dysfunction or liver tissue damage is aggravated gradually, but changes in liver energy metabolism and liver function occur prior to the morphologic changes in liver tissue.

Pathophysiological Mechanism of the Effect of Hypotensive Brain Death on Liver Function and Liver Tissue Morphology

Brain death, hypotension, and organ hypoperfusion. Brain death is a complex situation with an enormous number of variables affecting donor livers. Golling et al found in a pig brain death model that systemic perfusion parameters, intestinal ischemia (gastric mucosal pH and endotoxin levels), and oxidative stress were affected by hemodynamic status and that portal vein blood flow, hepatic microcirculation, liver cell damage, endotoxin removal ability, and the deterioration of liver oxidative stress were not affected by hemodynamic status [24]. Van der Hoeven et al found that maintaining normal blood pressure after brain death could reduce the severity of a specific hepatocellular dysfunction, but it could not completely prevent other functional disorders associated with brain death [20]. McCuskey et al found that hypotension could lead to obvious gastrointestinal ischemia and was associated with intestinal mucosal permeability increase and endotoxin displacement, which eventually led to liver dysfunction [25].

In this study, portal vein and hepatic arterial blood flow monitoring showed that the liver and gastrointestinal tract presented a low perfusion state under hypotensive brain death. Under the state of brain death, hemodynamic abnormalities and low perfusion of the liver and intestines may impair the donor liver through direct and/or indirect pathways.

Release of Endotoxin and Cytokine Damage Hepatocytes

Endotoxins are lipopolysaccharides in the cell wall of gram-negative bacteria that largely exist in the intestinal tract. Under physiological conditions, the close connection of intestinal mucosa cells can prevent endotoxins from entering the bloodstream. However, damage to the intestinal mucosal barrier can cause enterogenous endotoxin blood disease. Endotoxins have a wide range of biological activities and can damage donor livers through various direct and/or indirect mechanisms [26]. In the present study, the portal vein endotoxin level increased gradually under the state of hypotensive brain death, suggesting that the state of hypotensive brain death may harm the intestinal mucosal barrier. This can lead to intestinal endotoxins entering the bloodstream and eventually contribute to liver injury.

Endotoxins are one of the most important substances that can activate Kupffer cells. Activated Kupffer cells can damage the donor liver by producing reactive oxygen radicals, promoting local anoxia of the liver sinus, and producing various inflammatory cytokines (eg, TNF-α and IL-1) [7,27]. Zhang et al found in a rabbit brain death model

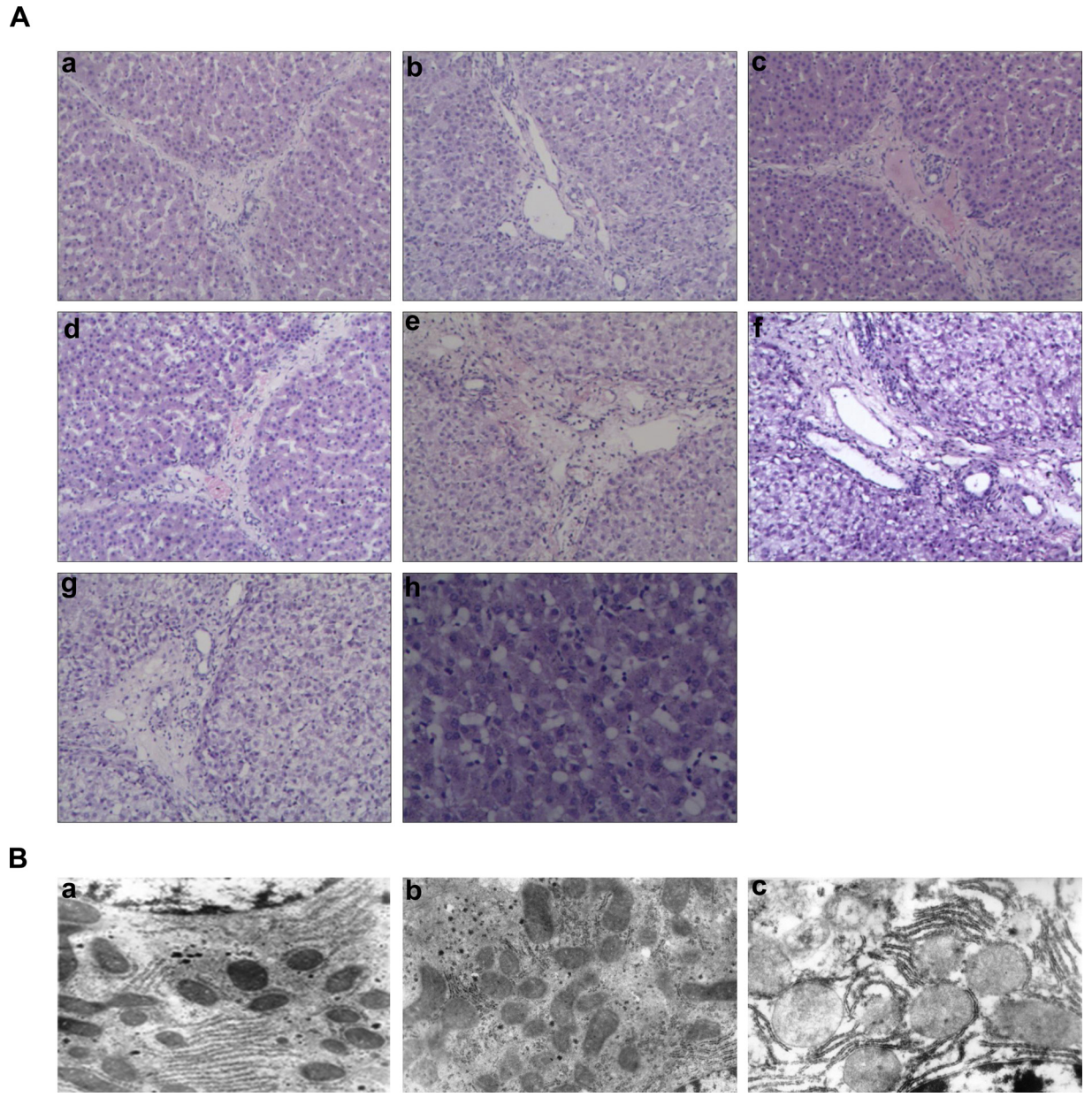

Fig 5. Changes in liver tissue morphology. (A) Liver tissue hematoxylin-eosin (H&E) staining (a-h: baseline, T1, T2, T3, T4, T5, T7, and T12). (B) Liver tissue electron microscopy images (a-c: baseline, T3, and T12).

that the activation of Kupffer cells may be related to damage of brain death donor livers and that inhibiting the activity of Kupffer cells could protect donor livers [7]. In the present study, both endotoxin and inflammatory factors increased gradually under the state of hypotensive brain death; thus, we hypothesize that endotoxin release caused by hypotensive brain death activates Kupffer cells and that activated Kupffer cells damage donor liver cells through multiple mechanisms, including the release of inflammatory factors.

Effect of the Increase in ET-1 Level and Decrease in NO Level on Liver Microcirculation Disorders

Endothelin is an active peptide with strong contractile vasculature and 3 isoforms, namely ET-1, ET-2, and ET-3, among which ET-1 has the strongest activity. The hepatic and portal vein system has abundant endothelin receptors, so ET-1 has an important regulatory effect on the hemodynamics of the liver and portal vein system. An increase in ET-1 level has many adverse effects on the liver, including hepatic sinus contraction, decreased perfusion rate,

increased portal vein pressure, and increased vascular resistance in the liver [28]. NO is a unique multieffect messenger molecule, and endothelial cell source NO has strong vasodilation properties, which can regulate blood pressure and regional blood flow. A low level of NO, one of the main cytokines regulating liver microcirculation, can antagonize contractile regulation factors, such as ET-1 and platelet-activating factor, and prevent endothelin and thrombin A2 expression. In addition, NO can protect the liver by reducing the activity of inflammatory cells, inhibiting the expression of cytokines and adhesion molecules, and inhibiting the apoptosis of hepatocytes [29].

The hepatic microvascular system consists of the portal vein, hepatic artery, hepatic sinus, central vein, and lymphatic vessels, of which, the hepatic sinus is a key regulator of hepatic microcirculation flow. The hepatic stellate cell, located in the space of Disse of endothelial cells, is an important factor for regulating the size of the hepatic sinus, whereas ET-1 and NO can regulate the microcirculation of the liver by regulating the contraction and diastolic effect of the hepatic stellate cell [30]. This study found that the state of hypotensive brain death could cause an increase in ET-1 level, decrease in NO level, and ET-1 and NO imbalances. These changes can lead to increased hepatic sinus contractility and decreased hepatic microcirculation vascular bed capacity, resulting in microcirculation disorder and a reduction of the protective effect of NO on the liver.

Decreased Hepatic HIF-1α Aggravates Hepatic Anoxia Damage

Hypoxia-inducible factor 1 is a nuclear transcription factor consisting of 2 subunits, α and β, and is produced as a cell adaptation to hypoxia. The β subunit, located in the nucleus, is relatively stable and not affected by cell oxygen partial pressure. The α subunit is located in the cytoplasm and quickly degrades when cells are fully oxygenated. When the oxygen partial pressure of cells decreases, HIF-1α accumulates and transfers from the cytoplasm to the nucleus. The combination of α and β subunits form active HIF-1, which initiates a series of gene expressions that induce cells to adapt to hypoxia and makes them become more resistant to anoxia [31,32]. Guo et al found that stability treatment with HIF-1α could reduce liver ischemia-reperfusion injury and that HIF-1α played an important role in the acute phase of hepatic ischemia or hypoxia [33]. Zhang et al found that the use of FG-4592 in the pretreatment of DCDs to enhance HIF-1 activity could upregulate protective gene expression and reduce liver thermal ischemia and cryopreservation injury [32]. This study found that hypotensive brain death could inhibit the increase in HIF-1α response, which may lead to intolerance of the liver to decreased hypoxia and further aggravate liver damage.

Limitations

The main limitations of this study are that the effects of simple brain death or simple hypotension on the donor liver were not observed, and this study adopted self-controlled grouping, which weakened the persuasiveness of this research to some extent.

CONCLUSIONS

In this study, a hypotensive brain death pig model was successfully established using an improved intracranial water sac inflation method. Hepatic injury was found to be progressively aggravated under the state of hypotensive brain death. The mechanism of donor liver injury under the state of hypotensive brain death may involve low liver perfusion, release of intestinal endotoxin, release of inflammatory factors (eg, TNF-α and IL-1), decreased HIF-1α level, and ET-1 and NO imbalance.

ACKNOWLEDGMENTS

This research was performed at the Key Laboratory of Organ Transplantation, Tianjin First Center Hospital. This work was supported by the National Natural Science Foundation of China (grant no. 81272547) and Tianjin Science and Technology Project (grant no. 15ZXLCSY00040).

REFERENCES

[1] Scalea JR, Redfield RR, Foley DP. Liver transplant outcomes using ideal donation after circulatory death livers are superior to using older donation after brain death donor livers. Liver Transpl 2016;22:1197–204.

[2] Bozkurt B, Dayangac M, Tokat Y. Living donor liver transplantation. Chirurgia 2017;112:217–28.

[3] Ausania F, White SA, Coates R, Hulme W, Manas DM. Liver damage during organ donor procurement in donation after circulatory death compared with donation after brain death. British J Surg 2013;100:381–6.

[4] Rai R. Liver transplantatation- an overview. Indian J Surg 2013;75:185–91.

[5] Bugge JF. Brain death and its implications for management of the potential organ donor. Acta Anaesthesiol Scand 2009;53:1239–50.

[6] Jimenez-Castro MB, Gracia-Sancho J, Peralta C. Brain death and marginal grafts in liver transplantation. Cell Death Dis 2015;6:e1777.

[7] Zhang SJ, Shi JH, Tang Z, Wu Y, Chen S. Protective effects of glycine pretreatment on brain-death donor liver. Hepatobiliary Pancreat Dis Int 2005;4:37–40.

[8] Machado C, Perez-Nellar J, Estevez M, Gonzalez E. Evidence-based guideline update: determining brain death in adults: report of the Quality Standards Subcommittee of the American Academy of Neurology. Neurology 2011;76:307 [author reply 308-9].

[9] Brain Injury Evaluation Quality Control Centre of National Health, Family Planning Comission. Criteria and practical guidance for determination of brain death in adults (BQCC version). Chin Med J 2013;126:4786–90.

[10] Bruinsma GJ, Nederhoff MG, van de Kolk CW, et al. Bioenergetic response of the heart to dopamine following brain death-related reduced myocardial workload: a phosphorus-31 magnetic resonance spectroscopy study in the cat. J Heart Lung Transplant 1999;18:1189–97.

[11] Chiari P, Piriou V, Hadour G, et al. Preservation of ischemia and isoflurane-induced preconditioning after brain death in rabbit hearts. Am J Physiol Heart Circ Physiol 2002;283:H1769–74.

[12] Watts RP, Bilska I, Diab S, et al. Novel 24-h ovine model of brain death to study the profile of the endothelin axis during cardiopulmonary injury. Intensive Care Med Exp 2015;3:31.
[13] Bozovic G, Steen S, Sjoberg T, et al. Circulation stabilizing therapy and pulmonary high-resolution computed tomography in a porcine brain-dead model. Acta Anaesthesiol Scand 2016;60: 93–102.
[14] Esmaeilzadeh M, Sadeghi M, Galmbacher R, et al. Time-course of plasma inflammatory mediators in a rat model of brain death. Transpl Immunol 2017;43-4:21–6.
[15] Chen L, Feng X, Wang Y, et al. Study of the role of transforming growth factor beta-1 in organ damage protection in porcine model of brain death. Transplant Proc 2016;48:205–9.
[16] Zens TJ, Danobeitia JS, Chlebeck PJ, et al. Guidelines for the management of a brain death donor in the rhesus macaque: a translational transplant model. PLoS One 2017;12:e0182552.
[17] Purins K, Sedigh A, Molnar C, et al. Standardized experimental brain death model for studies of intracranial dynamics, organ preservation, and organ transplantation in the pig. Crit Care Med 2011;39:512–7.
[18] Purins K, Enblad P, Wiklund L, Lewen A. Brain tissue oxygenation and cerebral perfusion pressure thresholds of ischemia in a standardized pig brain death model. Neurocrit Care 2012;16:462–9.
[19] Li S, Korkmaz-Icoz S, Radovits T, et al. Donor preconditioning after the onset of brain death with dopamine derivate n-octanoyl dopamine improves early posttransplant graft function in the rat. Am J Transplant 2017;17:1802–12.
[20] van Der Hoeven JA, Ter Horst GJ, Molema G, et al. Effects of brain death and hemodynamic status on function and immunologic activation of the potential donor liver in the rat. Ann Surg 2000;232:804–13.
[21] Novitzky D, Cooper DK, Morrell D, Isaacs S. Change from aerobic to anaerobic metabolism after brain death, and reversal following triiodothyronine therapy. Transplantation 1988;45:32–6.
[22] Olinga P, van der Hoeven JA, Merema MT, Freund RL, Ploeg RJ, Groothuis GM. The influence of brain death on liver function. Liver Int 2005;25:109–16.
[23] van der Hoeven JA, Ploeg RJ, Postema F, et al. Induction of organ dysfunction and activation of inflammatory markers in donor liver and kidney during hypotensive brain death. Transplant Proc 1999;31:1006–7.
[24] Golling M, Mehrabi A, Blum K, et al. Effects of hemodynamic instability on brain death-induced prepreservation liver damage. Transplantation 2003;75:1154–9.
[25] McCuskey RS, Urbaschek R, Urbaschek B. The microcirculation during endotoxemia. Cardiovasc Res 1996;32:752–63.
[26] Nolan JP. Endotoxin, reticuloendothelial function, and liver injury. Hepatology 1981;1:458–65.
[27] Bilzer M, Roggel F, Gerbes AL. Role of Kupffer cells in host defense and liver disease. Liver Int 2006;26:1175–86.
[28] Palmes D, Budny TB, Stratmann U, Herbst H, Spiegel HU. Endothelin-A receptor antagonist reduces microcirculatory disturbances and transplant dysfunction after partial liver transplantation. Liver Transpl 2003;9:929–39.
[29] Abu-Amara M, Yang SY, Seifalian A, Davidson B, Fuller B. The nitric oxide pathway–evidence and mechanisms for protection against liver ischaemia reperfusion injury. Liver Int Liver 2012;32: 531–43.
[30] Rockey DC. Hepatic blood flow regulation by stellate cells in normal and injured liver. Semin Liver Dis 2001;21:337–49.
[31] Brahimi-Horn MC, Pouyssegur J. HIF at a glance. J Cell Sci 2009;122:1055–7.
[32] Zhang X, Liu Z, Xiao Q, et al. Donor treatment with a hypoxia-inducible factor-1 agonist prevents donation after cardiac death liver graft injury in a rat isolated perfusion model. Artif Organs 2018;42:280–9.
[33] Guo Y, Feng L, Zhou Y, et al. Systematic review with meta-analysis: HIF-1α attenuates liver ischemia-reperfusion injury. Transplant Rev 2015;29:127–34.